RADIATION RESEARCH **193**, 000–000 (2019)
0033-7587/19 $15.00

DOI: 10.1667/RR15491.1

UVC-Emitting $LuPO_4:Pr^{3+}$ Nanoparticles Decrease Radiation Resistance of Hypoxic Cancer Cells

Matthias Müller,[a] Sara Espinoza,[c] Thomas Jüstel,[c] Kathryn D. Held,[b] R. Rox Anderson[a] and Martin Purschke[a,1]

[a] *Wellman Center for Photomedicine and* [b] *Department of Radiation Oncology, Massachusetts General Hospital/Harvard Medical School, Boston, Massachusetts; and* [c] *Department of Chemical Engineering, Münster University of Applied Sciences, Steinfurt, Germany*

Müller, M., Espinoza, S., Jüstel, T., Held, K. D., Anderson, R. R. and Purschke, M. UVC-Emitting $LuPO_4:Pr^{3+}$ Nanoparticles Decrease Radiation Resistance of Hypoxic Cancer Cells. ***Radiat. Res.*** **193, 000–000 (2019).**

Radiation-resistant hypoxic tumor areas continue to present a major limitation for successful tumor treatment. To overcome this radiation resistance, an oxygen-independent treatment is proposed using UVC-emitting $LuPO_4:Pr^{3+}$ nanoparticles (NPs) and X rays. The uptake of the NPs as well as their effect on cell proliferation was investigated on A549 lung cancer cells by using inverted time-lapse microscopy and transmission electron microscopy. Furthermore, cytotoxicity of the combined treatment of X rays and $LuPO_4:Pr^{3+}$ NPs was assessed under normoxic and hypoxic conditions using the colony formation assay. Transmission electron microscopy (TEM) images showed no NP uptake after 3 h, whereas after 24 h incubation an uptake of NPs was documented. $LuPO_4:Pr^{3+}$ NPs alone caused a concentration-independent cell growth delay within the first 60 h of incubation. The combined treatment with UVC-emitting NPs and X rays reduced the radiation resistance of hypoxic cells by a factor of two to the level of cells under normoxic condition. $LuPO_4:Pr^{3+}$ NPs cause an early growth delay but no cytotoxicity for the tested concentration. The combination of these NPs with X rays increases cytotoxicity of normoxic and hypoxic cancer cells. Hypoxic cells become sensitized to normoxic cell levels.

INTRODUCTION

Cancer is a major cause of mortality worldwide. In 2018, there were an estimated 18.1 million new cancer cases and 9.6 million deaths attributed to cancer (*1*). Currently, radiation therapy is the gold standard for many inoperable malignant tumors. Nearly 50% of patients with solid tumors undergo radiation therapy during the course of their disease (*2*). For the successful outcome of the treatment, the oxygen level within regions of the tumor microenvironment plays a crucial role. Hypoxic areas of the tumor are more radiation resistant and are thought to be responsible for poor treatment outcome, formation of metastasis and tumor recurrence (*3–5*). Currently, fractionated irradiation and complex treatment plans are employed to overcome radiation resistance and minimize side effects.

Combining nanoparticles (NPs) as radiosensitizers with X rays is a promising approach for increasing tumor control. In particular, gold NPs have been shown to increase the local dose of ionizing radiation at the tumor site, causing increased DNA damage (*6–9*). The high atomic number of gold ($Z = 79$) provides a large absorption cross section for X-ray irradiation, which leads to emission of radiation of lower energy but higher absorbance in tissue. Nevertheless, the mechanism of the generation of DNA damages using gold NPs and X rays still relies on oxygen and their effect is reduced by tumor hypoxia (*10*).

This study focused on the reduction of the radiation resistance of hypoxic cancer cells. Unlike ionizing radiation, ultraviolet (UV) radiation between 200 and 300 nm targets cellular DNA directly via an oxygen-independent mechanism (*11–14*). We combined traditional X-ray irradiation with the UV-emitting scintillator $LuPO_4:Pr^{3+}$ to generate localized UV photons at the cellular level. $LuPO_4:Pr^{3+}$ efficiently converts X rays into UV radiation due to interconfigurational $[Xe]4f^15d^1$-$[Xe]4f^2$ ($^3F_2$, $^3H_6$, $^3H_5$, $^3H_4$-terms) transitions of Pr^{3+} resulting in four narrow emission bands in the range of 220–285 nm (*15, 16*).

Ultraviolet radiation produces two major types of DNA damage, cyclobutane pyrimidine dimers (CPDs) and 6–4 photoproducts, which can lead to permanent cell cycle arrest followed by cell inactivation (*13, 17, 18*). UV photons are strongly absorbed within a few micrometers, so that only cells in the immediate vicinity of NPs would be affected, while surrounding healthy tissue would be spared (*19*). Due to fenestrated blood vessels within the cancer which result in enhanced permeability and retention (EPR effect), intravenously-injected NPs accumulate preferentially in solid tissue tumors (*20*). *In vitro* experiments were performed to test the hypothesis that UV-scintillating NPs can radiosensitize cells under normoxic and hypoxic conditions.

[1] Address for correspondence: Wellman Center for Photomedicine, Their 201A, Massachusetts General Hospital/Harvard Medical School, 40 Blossom St., Boston, MA 02114; email: mpurschke@mgh.harvard.edu.

MATERIALS AND METHODS

Preparation of $LuPO_4$:Pr^{3+}

$LuPO_4$:Pr^{3+} particles were obtained from Radiation Monitoring Devices, Inc. (Watertown, MA). The particles were synthesized via a coprecipitation method as described elsewhere (*21*). For cell experiments, the particles were dispersed in Dulbecco's modified Eagle's medium (DMEM; Gibco, Grand Island, NY). Darvan C (0.01%) was added to prevent agglomeration of the particles in the media. The mixture was blended thoroughly and subsequently sonicated for 15 min. The particle dispersion was freshly prepared immediately prior to the experiment.

Cell Culture

Experiments were performed using the lung cancer cell line A549 (ATCC®, Manassas, VA). Cells were cultured in DMEM supplemented with 1% Pen/Strep (10,000 U × ml^{-1} penicillin, 10,000 mg × ml^{-1} streptomycin; Life Technologies, Carlsbad, CA) and 10% fetal bovine serum (Life Technologies) in a humidified incubator at 37°C. The atmosphere was regulated to 95% air and 5% CO_2. Cells were used in passages between 3 and 20.

X-Ray Irradiation and Colony Formation Assay

Cells (200,000) were seeded in 12.5 cm^2 flasks 24 h before the experiment. On the day of the experiment, cells were treated with the NPs and incubated in a hypoxic chamber for 4 h. The chamber was flushed with a N_2/CO_2 mixture (95%/5%) during the incubation. The oxygen content of the media in the hypoxic chamber was measured using the oxygen meter Fibox 4 trace (PreSens Precision Sensing GmbH, Regensburg, Germany) equipped with the oxygen sensor spot SP-PSt6-NAU in the media. After incubation, the cells were irradiated in the hypoxic chamber. Normoxic cells were treated the same way but were incubated under normal cell culture condition (air/CO_2 = 95%/5%). After X-ray irradiation, cells were gently washed with media to remove the NPs. Subsequently, cells were trypsinized, counted and reseeded in triplicates into six-well plates. The cells were incubated for 14 days in a humidified incubator at 37°C and 95% air and 5% CO_2. The cells were fixed for 30 min using 10% phosphate buffered formalin solution (pH = 6.9; Fisher Scientific™, Pittsburgh, PA) and stained with crystal violet solution (1 mg × ml^{-1}, ACS grade; MP Biomedicals, Santa Ana, CA).

X-Ray Irradiator

The samples were irradiated using the biological X-RAD 320 (Precision X-ray Inc., North Branford, CT) at a dose rate of 450 cGy × min^{-1}. Acceleration voltage and tube current were 320 kV and 12.5 mA, respectively. A 2-mm aluminum filter was used to harden the X-ray beam.

Transmission Electron Microscope (TEM) Imaging

Cells were incubated with and without particles for 3 and 24 h. After incubation, cells were fixed in Karnovsky fixative (K2 buffer). After washing the cells with the wash buffer, cells were treated with 1% OsO_4 at 4°C on an orbital shaker for 2 h. Subsequently, cells were gently collected and centrifuged to form a pellet. Warm agar was added to the pellet to form an agar-cell pellet. The agar-cell pellet was then dehydrated, in gradient alcohol series, infiltrated with propylene oxide/Epon t812 gradient mix and embedded in Epon t812 (Tousimis®, Rockville, MD). Semi-thin sections (0.5 μm) were cut and stained with Toluidine blue. Ultrathin sections (80 nm) were cut using a Reichert-Jung Ultracut E microtome (Vienna, Austria), collected on uncoated 100-mesh copper grids, stained with 2% uranyl acetate and lead citrate, (2.66% lead nitrate, 3.52% sodium citrate) and examined on a Philips CM-10 transmission electron microscope (Eindhoven, The Netherlands). Digital TEM images were taken using an AMT-XR41M 4.0 Megapixel Cooled sCMOS camera (Advanced Microscopy Techniques, Woburn, MA).

Time-Lapse Imaging

Cell growth within the first 60 h was investigated using the inverted microscope Axio Observer Z1 (Carl Zeiss, Jena, Germany) equipped with the Axiocam 702 mono camera (Carl Zeiss) as well as with a temperature- and atmosphere-controlled, humidified chamber. The temperature was 37°C and the atmosphere was set to 95% air and 5% CO_2. One day before the experiment, 2,000 cells were seeded into each well of a 12-well plate. Immediately before the experiment, cells were treated with the NPs. Images were taken every 15 min over the course of 60 h. The cell number was determined manually by counting the cells in a randomly selected 1,069 μm × 677 μm section.

Calculation of the Oxygen Enhancement Ratios

To quantify the cytotoxic effect of the combined treatment under hypoxia, the oxygen enhancement ratio (OER) was calculated. The OER describes the enhancement of a therapeutic effect of ionizing radiation due to the presence of oxygen and is defined as:

$$OER = \frac{D_{10}\ hypoxia}{D_{10}\ normoxia}. \quad (1)$$

OERs were calculated for the dose at which 10% of the cells survived (D_{10}). Therefore, D_{10} values were determined by fitting each survival dataset to the linear-quadratic model:

$$y = y_0 \times \exp(-\alpha x - \beta x^2). \quad (2)$$

In Eq. (2), y and y_0 are the surviving fraction at a certain time as well as the initial surviving fraction at timepoint 0, x is the X-ray dose and α and β are arbitrary fitting parameters.

Statistical Analysis

All experiments were performed using at least three independent replicates. The results are presented as mean ± standard error of mean. For statistical analysis GraphPad Prism software version 8.1.1 for Windows (La Jolla, CA) was used. Statistically significant differences were calculated using two-way analysis of variance (ANOVA) corrected by Tukey's multiple comparisons test. $P < 0.05$ was considered to be statistically significant.

RESULTS

Localization of the Particles within A549 Cells

TEM images were taken to investigate NP uptake by the cells. Figure 1 shows the TEM images of A549 cells incubated with $LuPO_4$:Pr^{3+} for 3 and 24 h. The images did not show large agglomerates of the $LuPO_4$:Pr^{3+} particles but small clusters of particles were observed. After 3 h incubation, the particles were accumulated outside of the cells along the cell membrane. After 24 h incubation, cellular uptake was observed with clusters of particles in close proximity to the cell nucleus.

Effect of the Cytotoxicity of $LuPO_4$:Pr^{3+} on Cell Growth

To determine the effect of the NPs on cell proliferation, cells were incubated with NPs and the cell number was assessed every 12 h. Figure 2 shows the cellular

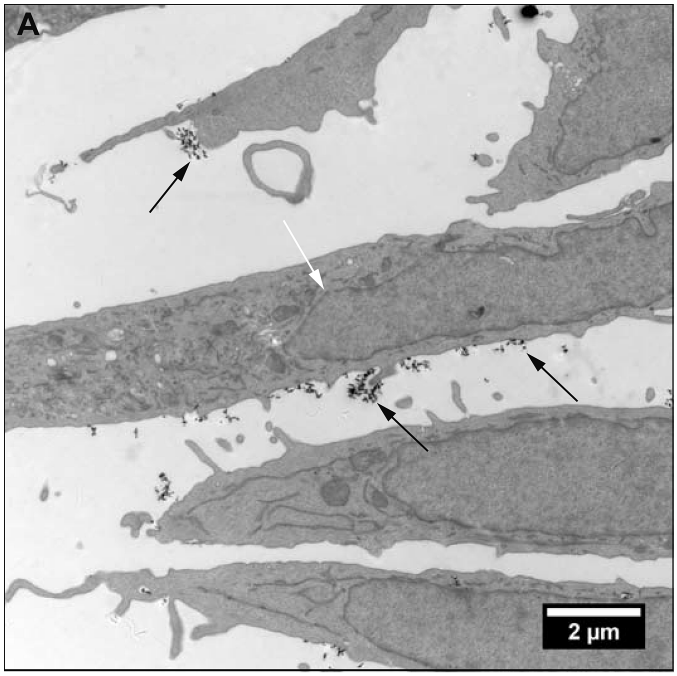

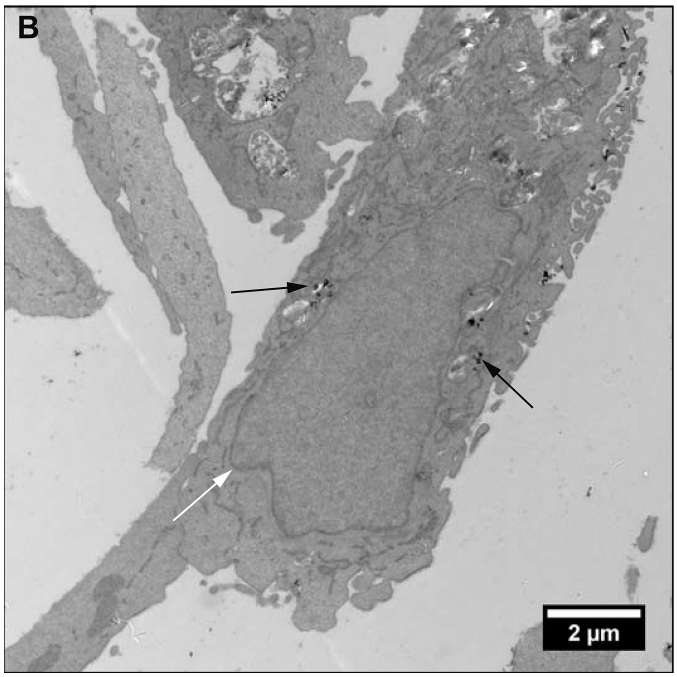

FIG. 1. TEM images of A549 cells incubated with $LuPO_4:Pr^{3+}$ after 3 and 24 h (panels A and B, respectively) at 1,900× magnification. Black arrows indicate NPs and white arrows indicate nuclei.

proliferation of A549 cells over 60 h incubated with 0, 0.1, 0.25 and 1.0 mg × ml^{-1} $LuPO_4:Pr^{3+}$ under normoxic conditions. The cell number of the untreated control increased eightfold within 60 h. Statistically significant differences in the cell numbers were observed at all timepoints for the control cells. Cells treated with NPs showed a slower growth (sixfold), which was independent of the tested NP concentrations. However, no significant

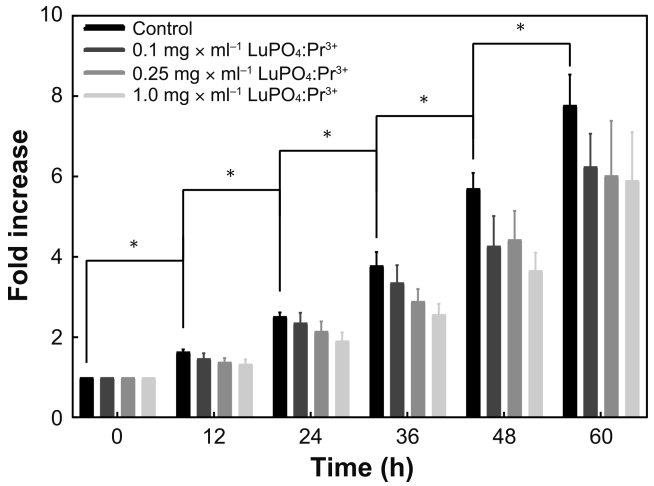

FIG. 2. Cell counts of A549 cells after incubation under normoxic conditions with 0, 0.1, 0.25 and 1.0 mg × ml^{-1} $LuPO_4:Pr^{3+}$ at different timepoints. Data results from five independent experiments and error bars represent standard error of mean.

difference in the cell number for the control and treated cells was found after 60 h.

Cytotoxic Effect of the Combined Treatment of Hypoxic A549 Cells

To confirm the hypoxic atmosphere of the cell environment, the oxygen content was measured. Figure 3 shows the volume fraction of oxygen in the atmosphere and the cell culture media over time, while the hypoxic chamber was flushed with N_2/CO_2 (95%/5%). The oxygen concentration in the atmosphere decreased to 0.05% within 15 min, whereas the oxygen concentration in the media decreased to a minimum of 0.2% at 120 min.

To evaluate the cytotoxicity of the combined treatment under hypoxic conditions, clonogenic survival of normoxic and hypoxic A549 cells was compared. Figure 4 shows the survival curves of A549 cells X-ray irradiated with and without $LuPO_4:Pr^{3+}$ NPs. The fitting parameters (α, β) and the coefficient of determination (R^2) are summarized in Table 1. The surviving fractions of the control as well as of treated cells decreased with increasing X-ray dose. The black curves represent the surviving fraction of cells incubated with 0, 2.5 and 5.0 mg × ml^{-1} $LuPO_4:Pr^{3+}$ NPs for 4 h under normoxic conditions. The clonogenic survival of the untreated control decreased to 1.3% after 12 Gy X-ray irradiation. For NP concentrations of 2.5 and 5.0 mg × ml^{-1}, the surviving fraction for 12 Gy X-ray irradiated cells decreased further to 0.04% and 0.02%, respectively. The survival curves of the hypoxic cells are indicated by the gray curves. The surviving fraction of the hypoxic control decreased to 17% at a radiation dose of 12 Gy. The clonogenic survival of the hypoxic cells treated with 2.5 and 5.0 mg × ml^{-1} $LuPO_4:Pr^{3+}$ decreased to 2.2 and 1.2% for 12 Gy irradiation.

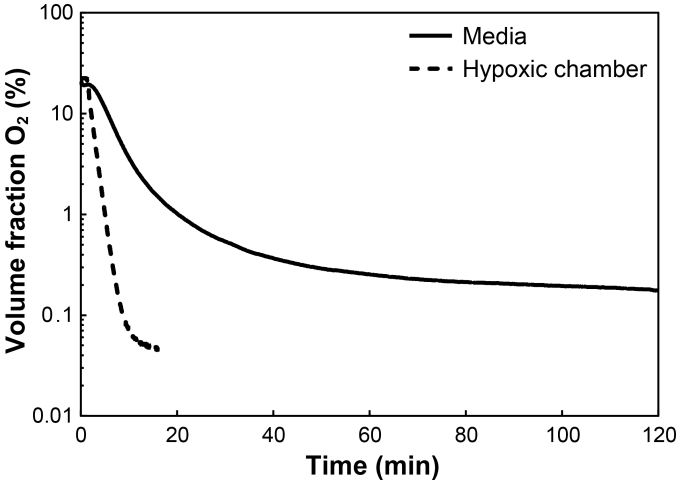

FIG. 3. Volume fraction of O_2 in the gas phase of the chamber as well as in the cell culture media.

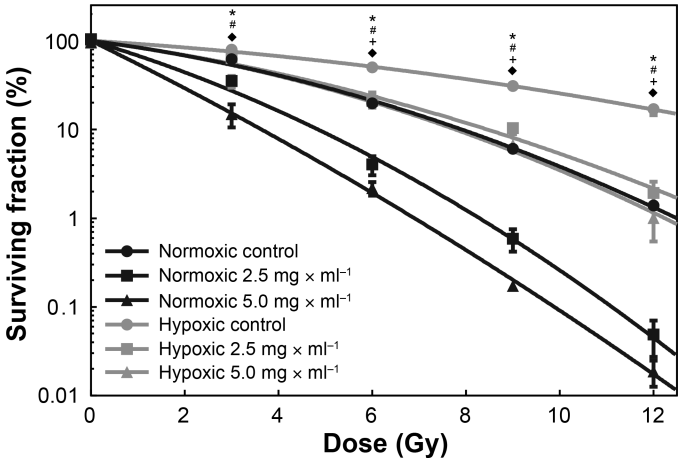

FIG. 4. Cell survival of A549 cells under normoxic and hypoxic conditions incubated for 4 h with 0, 2.5 and 5.0 mg × ml^{-1} $LuPO_4$:Pr^{3+} and different X-ray doses. Statistically significant differences between normoxic control and 2.5 mg × ml^{-1} as well as 5.0 mg × ml^{-1} $LuPO_4$:Pr^{3+} are labeled as (*) and (#). Statistically significant differences between hypoxic control and 2.5 mg × ml^{-1} as well as 5.0 mg × ml^{-1} $LuPO_4$:Pr^{3+} are labeled as (+) and (◆). Each point represents data from at least three independent experiments and error bars represent standard error of mean.

The D_{10} values for the normoxic and hypoxic controls were calculated to be 7.9 and 14.2 Gy (Table 1). The latter value was extrapolated from data derived from the fitting function. The OER was calculated to be 1.8 at that survival level. Furthermore, the D_{10} values for 2.5 and 5.0 mg × ml^{-1} $LuPO_4$:Pr^{3+} were 4.8 Gy and 3.6 Gy for normoxic and 8.5 and 8.0 Gy for hypoxic samples. Therefore, the OER was calculated to be 1.8 for a concentration of 2.5 mg × ml^{-1} $LuPO_4$:Pr^{3+} and 2.2 for a concentration of 5.0 mg × ml^{-1} $LuPO_4$:Pr^{3+}at 10% survival.

DISCUSSION

Hypoxic tumor regions are challenging to treat with conventional radiation therapy due to the critical role of oxygen for the fixation of X-ray-induced DNA damages (*22, 23*). The oxygen-independent mechanism of UVC to produce DNA damages could be a promising tool to overcome radiation resistance of hypoxic regions. In a previously published study, we demonstrated increased cell death after the combined treatment of UVC NPs and X rays compared to X rays alone. We also confirmed the presence of UV-specific DNA damages for the combined treatment under normoxic condition (*16, 21, 24*). In the current study we showed that radiation resistance of normoxic and hypoxic A549 cells can be reduced by combining $LuPO_4$:Pr^{3+} NPs and X rays.

The distance of the NPs to the DNA is important for an efficient outcome of the combined approach. With decreasing distance between NPs and nucleus, the efficacy of the combined treatment is expected to increase. For our experiments we assume that the NPs were located mainly outside the cells as indicated by the TEM images (Fig. 1A). Within the first 3 h, no cellular uptake of the NPs was observed. Incubation time of 24 h showed an increased uptake of NPs (Fig. 1B), as evidenced by the TEM images taken after 24 h of incubation (Fig. 1B), which suggests an improved efficacy of the combined treatment for longer incubation periods prior to radiation. A549 cells incubated with 0.1, 0.25 and 1.0 mg × ml^{-1} $LuPO_4$:Pr^{3+} NPs were found to have a transient growth delay, which is expressed by a 25% slower growth rate within the first 60 h with no effect on cell survival (Fig. 2). Therefore, the slower proliferation of the treated cells did not lead to a significant difference in the cell number after 60 h compared to the control.

The cell culture experiments confirmed an increased cell death of normoxic and hypoxic A549 cells after the combined treatment with X rays and $LuPO_4$:Pr^{3+} NPs (Fig. 4). The decrease in radiation resistance became more distinct with increasing NP concentration. The tested concentrations of 2.5 mg × ml^{-1} and 5.0 mg × ml^{-1} $LuPO_4$:Pr^{3+} NPs reduced the surviving fraction of hypoxic A549 cells similar to the level of normoxic cells. The increasing α value with increasing NP concentration suggests a higher sensitivity to radiation, which is attributed to an increased generation of UVC radiation.

The OER values derived from the survival curves were 1.8, 1.8 and 2.2 for 0, 2.5 and 5.0 mg × ml^{-1} $LuPO_4$:Pr^{3+}, respectively. These numbers indicate an increased radiation resistance for the hypoxic A549 cells by a factor of approximately two in our experimental setup. As the OER values with and without NPs only show minor differences, it is concluded that the combined treatment of NPs and X rays sensitizes normoxic and hypoxic cells to the same extent.

In our experiments, the calculated OER values of approximately two indicate that the hypoxic cells are approximately twice as resistant as the normoxic cells.

TABLE 1
Fitting Parameters α, β and Coefficient of Determination R^2 Using the Linear-Quadratic Model as well as the Calculated D_{10} Values for Experimental Data Shown in Fig. 4

Condition	Sample	α (Gy^{-1})	β (Gy^{-2})	R^2	D_{10} (Gy)
Normoxic	Control	0.15 ± 0.02	0.017 ± 0.002	0.992	7.9
	2.5 mg × ml^{-1}	0.36 ± 0.05	0.023 ± 0.005	0.972	4.8
	5.0 mg × ml^{-1}	0.60 ± 0.03	0.010 ± 0.003	0.988	3.6
Hypoxic	Control	0.07 ± 0.01	0.006 ± 0.001	0.998	14.2
	2.5 mg × ml^{-1}	0.12 ± 0.04	0.017 ± 0.004	0.973	8.5
	5.0 mg × ml^{-1}	0.17 ± 0.06	0.017 ± 0.006	0.948	8.0

That is, the radiation-induced cytotoxic effect on the hypoxic cells is only 50% of the normoxic cells. Moreover, after 120 min incubation, the oxygen content in the culture media was below 0.2% (Fig. 3). These findings are in accordance with the literature, which describes these experimental conditions as radiobiological hypoxia. Radiobiological hypoxia is defined as the oxygen level at which the cytotoxic effect of radiation is half-maximal. Radiobiological hypoxia occurs at an oxygen concentration of approximately 0.4%, which is also the median O_2 content in prostate and pancreatic tumors (*25*). The difference between oxygen concentration derived from the OER and the measured concentration in the media is assigned to a rather slow oxygen exchange between the cells and the culture media (*26, 27*).

To increase the cellular uptake of the NPs as well as to avoid the clearance by the mononuclear phagocyte system in future experiments, clustering of the NPs must be minimized. Therefore, the size, shape and surface of the NPs need to be optimized by coating them with steric tumor targeting ligands. Steric stabilization of the NPs can be achieved using polyethylene glycol, polysaccharides or liposomes to encapsulate the NPs (*28, 29*). These coatings prevent the NPs from interacting with each other as well as interacting with immune cells (*30*). To deliver the NPs selectively to the tumor site, antibodies are well-established reagents for tumor targeting. For example, the epidermal growth factor receptor (EGFR) is expressed at significantly higher levels in epithelial cancers. As a result, NPs can be successfully delivered to the tumor by adding EGFR antibodies to the surface of the NP (*31*). Future experiments to investigate the cytotoxicity and efficacy will be performed in a 3D cell model as well as an animal model.

CONCLUSIONS

Radiation resistance of hypoxic A549 cancer cells can be decreased by a factor of two using the combined approach of UVC-emitting $LuPO_4:Pr^{3+}$ NPs and X rays. The oxygen-independent generation of UV-specific DNA damages reduces the surviving fraction of hypoxic A549 cells to the same level as their normoxic counterparts. In general, the effectiveness of radiation for both normoxic and hypoxic cells can be enhanced by applying $LuPO_4:Pr^{3+}$ NPs during X-ray irradiation. The observed effect of the combined treatment is mainly attributed to extracellularly located NPs due to their limited incubation time of 4 h. Longer incubation could increase the uptake and efficiency of the NPs.

ACKNOWLEDGMENTS

We are grateful to Yimin Wang and Michael R. Squillante from Radiation Monitoring Devices, Inc. for providing the $LuPO_4:Pr^{3+}$ NPs. We also thank H. Frederick Dylla and Ramtin Rahmanzadeh for fruitful discussions.

Received: August 12, 2019; accepted: October 21, 2019; published online: Month 0, 2019

REFERENCES

1. Bray F, Ferlay J, Soerjomataram I. Global Cancer Statistics 2018: GLOBOCAN estimates of incidence and mortality worldwide for 36 cancers in 185 countries. CA Cancer J Clin 2018; 68:394–424.
2. Delaney G, Jacob S, Featherstone C, Barton M. The role of radiotherapy in cancer treatment: Estimating optimal utilization from a review of evidence-based clinical guidelines. Cancer 2005; 104:1129–37.
3. Moeller BJ, Richardson RA, Dewhirst MW. Hypoxia and radiotherapy: Opportunities for improved outcomes in cancer treatment. Cancer Metastasis Rev 2007; 26:241–8.
4. Dunst J, Stadler P, Becker A, Lautenschlager C, Pelz T, Hansgen G, et al. Tumor volume and tumor hypoxia in head and neck cancers: The amount of the hypoxic volume is important. Strahlentherapie Onkol 2003; 179:521–6.
5. Sundfør K, Lyng H, Tropé CG, Rofstad EK. Treatment outcome in advanced squamous cell carcinoma of the uterine cervix: relationships to pretreatment tumor oxygenation and vascularization. Radiother Oncol 2000; 54:101–7.
6. Haume K, Rosa S, Grellet S, Smialek M, Butterworth K, Solov'yov A, et al. Gold nanoparticles for cancer radiotherapy: a review. Cancer Nanotechnol 2016; 7:1–20.
7. Her S, Jaffray DA, Allen C. Gold nanoparticles for applications in cancer radiotherapy: Mechanisms and recent advancements. Adv Drug Deliv Rev 2015; 109:84–101.
8. Chang MY, Shiau AL, Chen YH, Chang CJ, Chen HHW, Wu CL. Increased apoptotic potential and dose-enhancing effect of gold nanoparticles in combination with single-dose clinical electron beams on tumor-bearing mice. Cancer Sci 2008; 99:1479–84.
9. Butterworth KT, Coulter JA, Jain S, Forker J, McMahon SJ, Schettino G, et al. Evaluation of cytotoxicity and radiation enhancement using 1.9 nm gold particles: Potential application for cancer therapy. Nanotechnology 2010; 21:295101.
10. Cui L, Tse K, Zahedi P, Harding SM, Zafarana G, Jaffray DA, et al. Hypoxia and cellular localization influence the radiosensitizing effect of gold nanoparticles (AuNPs) in breast cancer cells. Radiat Res 2014; 182:475–88.

11. Cadet J, Sage E, Douki T. Ultraviolet radiation-mediated damage to cellular DNA. Mutat 2005; 571:3–17.

12. Yagura T, Makita K, Yamamoto H, Menck CFM. Biological sensors for solar ultraviolet radiation. Sensors 2011; 11:4277–94.

13. Douki T, Court M, Sauvaigo S, Odin F, Cadet J. Formation of the main UV-induced thymine dimeric lesions within isolated and cellular DNA as measured by high performance liquid chromatography-tandem mass spectrometry. J Biol Chem 2000; 275:11678–85.

14. Ben Said M, Otaki M. Development of a DNA-dosimeter system for monitoring the effects of pulsed ultraviolet radiation. Ann Microbiol 2013; 63:1057–63.

15. Srivastava AM, Jennings M, Collins J. The interconfigurational (4f15d1 → 4f2) luminescence of Pr3+ in LuPO4, K3Lu(PO4)2 and LiLuSiO4. Opt Mater (Amst) 2012; 34:1347–52.

16. Espinoza S, Volhard M, Katker H, Jenneboer H, Uckelmann A, Haase M, et al. Deep ultraviolet emitting scintillators for biomedical applications: the hard way of downsizing LuPO4:Pr3+. Part Part Syst Charact 2018; 35:1800282 (1–8).

17. Sinha RP, Hader D-P. UV-induced DNA damage and repair: a review. Photochem Photobiol Sci 2002; 1:225–36.

18. Yoon JH, Lee CS, O'Connor TR, Yasui A, Pfeifer GP. The DNA damage spectrum produced by simulated sunlight. J Mol Biol 2000; 299:681–93.

19. Anderson RR, Parrish JA. The optics of human skin. J Invest Dermatol 1981; 77:13–9.

20. Stylianopoulos T, Jain RK. Design considerations for nanotherapeutics in oncology. Nanomedicine 2015; 11:1893–907.

21. Squillante MR, Justel T, Anderson RR, Brecher C, Chartier D, Christian JF, et al. Fabrication and characterization of UV-emitting nanoparticles as novel radiation sensitizers targeting hypoxic tumor cells. Opt Mater (Amst) 2018; 80:197–202.

22. Ewing D. The oxygen fixation hypothesis: A reevaluation. Am J Clin Oncol 1998; 21:355–61.

23. Grimes DR, Partridge M. A mechanistic investigation of the oxygen fixation hypothesis and oxygen enhancement ratio. Biomed Phys Eng Express 2015; 1:045209.

24. Muller M, Wang Y, Squillante MR, Held KD, Anderson RR, Purschke M. UV scintillating particles as radiosensitizer enhance cell killing after X-ray excitation. Radiother Oncol 2018; 129:589–94.

25. Mckeown SR. Defining normoxia, physoxia and hypoxia in tumours – implications for treatment response. Br J Radiol 2014; 87:1–12.

26. Place TL, Domann FE, Case AJ. Limitations of oxygen delivery to cells in culture: An underappreciated problem in basic and translational research. Free Radic Biol Med 2017; 113:311–22.

27. Kurtcuoglu V, Scholz CC, Marti HH, Hoogewijs D. Frequently asked questions in hypoxia research. Hypoxia 2015; 3:35–43.

28. Valente I, Valle LJ, Casas MT, Franco L, Puiggali J. Nanospheres and nanocapsules of amphiphilic copolymers constituted by methoxypolyethylene glycol cyanoacrylate and hexadecyl cyanoacrylate units. Express Polym Lett 2013; 7:2–20.

29. Rahmanzadeh R, Rai P, Gerdes J, Hasan T. Targeted light-inactivation of the Ki-67 protein using theranostic liposomes leads to death of proliferating cells. Proc SPIE 2010; 7576:757602 (1–5).

30. Gon G, Tobias G. Nanooncology. 1st ed. Gon G, Tobias G, editors. Cham (CH): Springer; 2018.

31. Bazak R, Houri M, Achy S El, Kamel S, Officer H, Refaat T, et al. HHS public access. J Cancer Res Clin Oncol 2016; 141:769–84.